

Direct observation of the Ce 4*f* states in the Kondo semiconductor CeRhAs and related compounds: A high-resolution resonant photoemission study

Kenya Shimada,¹ Kenichi Kobayashi,² Takamasa Narimura,² Peter Baltzer,¹ Hirofumi Namatame,¹ Masaki Taniguchi,^{1,2} Toshiaki Suemitsu,³ Tetsuya Sasakawa,³ and Toshiro Takabatake³

¹Hiroshima Synchrotron Radiation Center, Hiroshima University, Higashi-Hiroshima 739-8526, Japan

²Graduate School of Science, Hiroshima University, Higashi-Hiroshima 739-8526, Japan

³Department of Quantum Matter, ADSM, Hiroshima University, Higashi-Hiroshima 739-8530, Japan

(Received 13 May 2002; revised manuscript received 5 July 2002; published 3 October 2002)

Ce 4*f* derived states at the Fermi level (E_F) of the isostructural single crystals CeRhAs, CeRhSb, and CePtSn were observed directly by means of high-resolution ($\Delta E = 18\text{--}20$ meV), low-temperature (10–12 K) photoemission spectroscopy with a photon energy of $h\nu = 126$ eV. The Ce 4*f* spectrum for the Kondo semiconductor CeRhAs exhibited no peak structure near E_F , and its spectral intensity decreases monotonically above the binding energy ~ 90 meV, thereby forming a large gap structure. The spectrum of the semimetal CeRhSb is enhanced above ~ 120 meV, but decreases steeply above ~ 13 meV, which indicates the existence of a narrow pseudogap at E_F . A clear crystal field excitation at ~ 27 meV, and a weak Kondo resonance at E_F , were found in the metal CePtSn.

DOI: 10.1103/PhysRevB.66.155202

PACS number(s): 71.28.+d, 71.27.+a, 75.30.Mb, 79.60.Bm

Among the highly correlated 4*f* electron systems, there are materials called Kondo semiconductors or semimetals, which have a small energy gap or pseudogap in the ground state without magnetic ordering.^{1,2} The temperature-dependent energy-gap formation cannot be explained within the framework of the single-impurity Anderson model (SIAM).³ The crossover from metallic states at high temperature to semiconducting or semimetallic states at low temperature occurs around a certain characteristic temperature, which is recognizable in the various transport and magnetic measurements.^{1,2} The temperature-dependent hybridization between the conduction bands and *f* states (*c-f* hybridization) near the Fermi level (E_F) has to be treated explicitly to explain the energy gap formation. This has been carried out on the basis of the periodic Anderson model (PAM), or the Kondo lattice model (KLM), with several computational methods.^{3–5}

CeRhAs and CeRhSb, with the orthorhombic ϵ -TiNiSi-type structure, are a Kondo semiconductor and Kondo semimetal, respectively.^{1,6,7} These compounds provide an ideal experimental system, since the difference of pnictogen leads to different transport properties. Recently, a single crystalline CeRhAs was grown.⁷ A broad peak in the magnetic susceptibility (χ) was found at $T_m \sim 500$ K.⁷ Anomalies at $T_1 = 370$ K, $T_2 = 235$ K, and $T_3 = 165$ K were observed in χ and the electrical resistivity (ρ).⁷ It was indicated that the energy-gap formation was closely coupled with lattice modulations.⁷

A broad maximum at ~ 120 K is found in χ and ρ for CeRhSb.⁶ The temperature-dependent tunneling spectroscopy of CeRhSb exhibited that the spectral intensity at E_F decreased below 23 K, forming a narrow V-shaped energy gap, $2\Delta_{p-p} \sim 20\text{--}27$ meV.⁸ The specific heat,⁹ as well as the $1/T_1$ in the NMR measurements,¹⁰ have been explained well by assuming a V-shaped pseudogap, with a halfwidth $\Delta = 28$ K,^{9,10} and a residual density of states at E_F .

Recently, Kumigashira *et al.* reported high-resolution temperature-dependent photoemission spectra for polycrys-

tals of CeRhSb and CeRhAs,^{11,12} with He resonance radiation (He I α : 21.218 eV and He II α : 40.814 eV). On the basis of the He II α -He I α difference spectra, the size of the pseudogap for the *f* states (Δ_f) as well as that for the conduction bands (Δ_c) were assumed to scale with the Kondo temperature (T_K), for both compounds.^{11,12} Also, they claimed that Δ_c 's were larger than Δ_f 's for both compounds.¹²

Although the difference-spectra of CeRhSb and CeRhAs deviated from that of metallic CePd₃ near E_F , the spectral intensities at E_F were high for both compounds.¹² The spectral features across E_F looked metallic and thus are inconsistent with the transport properties.¹²

We note that an accurate extraction of the Ce 4*f* spectra via the difference method is difficult in this case, since the photoionization cross-section of the Ce 4*f* orbital is smaller by one order of magnitude than that of the Rh 4*d* orbital in this photon energy region.¹³ Moreover, these experiments were conducted using scraped surfaces.^{11,12} Taking into account the surface sensitivity of photoemission spectra,¹⁴ it is obvious that the roughness of the scraped surface¹⁵ affects significantly the high-resolution photoemission spectral features.¹⁶

In this paper, we report high-resolution, low-temperature resonant photoemission spectra of CeRhAs and CeRhSb single crystals, and discuss unusual Ce 4*f* electronic states in these compounds. The Ce 4*f*-derived spectra are quite different from the previously reported difference-spectra.

We chose the isostructural Kondo metal CePtSn as a reference, which becomes antiferromagnetic below $T_N = 7.5$ K.^{17,18} The Ce 4*f* states were found to be well localized from clear crystal-field excitations observed at 20–30 meV in an inelastic neutron-scattering study.¹⁸

The Kondo temperatures for CeRhAs, CeRhSb, and CePtSn were estimated to be $T_K \sim 1500$ K (~ 130 meV), ~ 360 K (~ 30 meV), and ~ 10 K (< 1 meV),¹⁷ respectively. The former two temperatures were inferred by assum-

ing the relation $T_K \sim 3 T_m$.¹⁹ It should be noted that the unit-cell volume increases on going from CeRhAs (239 \AA^{-1}),²⁰ to CeRhSb (269 \AA^{-1}),²⁰ and to CePtSn (276 \AA^{-1}).¹⁷ The volume expansion should weaken the c - f hybridization.

CeRhAs and CeRhSb single crystals were grown by the Bridgman method,^{6,7} and CePtSn single crystals were grown by the Czochralski method.¹⁷ The transport and magnetic properties of the present samples are described elsewhere.^{6,7,17} Since impurities and/or defects have significant influences on the physical properties of Kondo semiconductors and Kondo semimetals,^{1,6} it is highly desirable to use single crystalline samples, especially for high-resolution photoemission measurements. In order to obtain clean surfaces, we fractured the single crystalline samples *in situ* in ultrahigh vacuum (3×10^{-10} Torr) at 10–12 K. The present measurements were carried out on a high-resolution linear undulator beamline (BL-1) connected to the compact electron-storage ring (HiSOR) located at Hiroshima Synchrotron Radiation Center (HSRC), Hiroshima University.²¹ The beamline is equipped with a high-resolution, hemispherical electron analyzer (SCIENIA ESCA200). The total instrumental energy resolution was set at 18–20 meV at $h\nu = 126$ eV. This was confirmed by the photoemission spectra of the Fermi edge of evaporated Au cooled at 10–12 K. The value of E_B is defined to E_F , which was calibrated using the Fermi edge of Au with the accuracy of ± 2 meV. Surface cleanliness was checked by using the spectral feature around 6 eV, which is sensitive to oxygen contamination. We performed angle-integrated photoemission spectroscopy by collecting photoelectrons emitted normally with acceptance angles of $\pm 6^\circ$ and $\pm 1.3^\circ$ along and perpendicular to the analyzer slit, respectively.²² We confirmed that the spectral features were highly reproducible. At photon energy of $h\nu = 126$ eV, which is close to the Ce $4d$ - $4f$ photoemission resonance peak at 122 eV, the Ce $4f$ contribution is enhanced significantly, and dominates the spectra. The Ce $4f^1$ -derived spectral shapes taken at $h\nu = 126$ eV do not differ from those taken at $h\nu = 122$ eV. Here we used $h\nu = 126$ eV for a lower background above E_F . The off-resonance spectra of these compounds taken at $h\nu = 115$ eV (not shown) have almost flat spectral shapes above $E_B \sim 2$ eV, and have a much weaker intensity compared with those taken at $h\nu = 126$ eV.

Figure 1 shows photoemission spectra of CeRhAs, CeRhSb, and CePtSn, taken at $h\nu = 126$ eV. Features at $E_B \sim 2$ – 2.5 eV correspond to the Ce $4f^0$ (Ce $4f^1 \rightarrow$ Ce $4f^0$) final states, and those above ~ 500 meV to the Ce $4f^1$ (Ce $4f^1 \rightarrow$ Ce $4f^1_c$) final states.²³ Here c denotes holes in the wide conduction bands. Analyses of the Ce $3d$ - $4f$ and $4d$ - $4f$ resonant photoemission spectra show that the surface and bulk contributions are dominant to the spectral weights of the Ce $4f^0$ and Ce $4f^1$ final states, respectively.²⁴ Here we concentrate on a discussion of the Ce $4f^1$ spectra very close to E_F . Spectral features shown by vertical bars for CePtSn are due to the Pt $5d$ states.

Figure 2 shows the Ce $4f^1$ -derived spectra. The intensities are normalized to the peak at ~ 300 meV. The Ce $4f^1$ spectra of CeRhSb and CePtSn are split by the spin-orbit

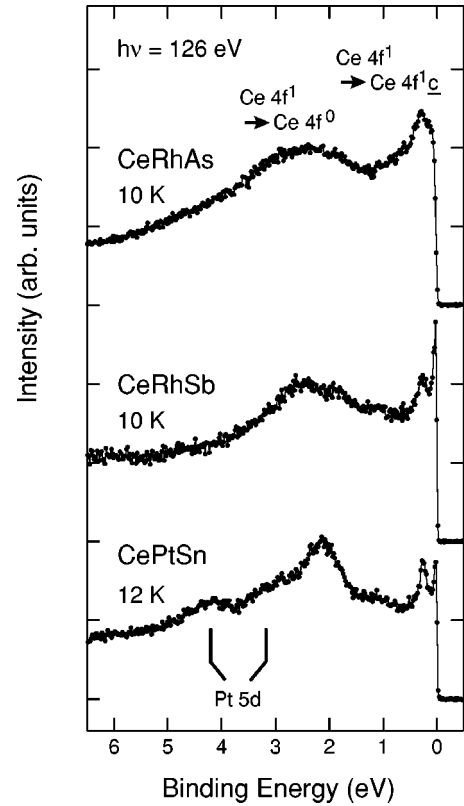


FIG. 1. High-resolution photoemission spectra of CeRhAs, CeRhSb, and CePtSn taken at $h\nu = 126$ eV at 10–12 K. The spectral intensities are normalized to the intensity of Ce $4f^0$ states at ~ 2 – 2.5 eV. Bars indicate Pt $5d$ -derived spectral features in CePtSn.

interaction into two peaks at ~ 300 meV and $\sim E_F$. Based on the SIAM, the spectral features at $\sim E_F$ are due either to a Ce $4f_{5/2}^1$ contribution, or to the tail of the Kondo resonance (KR), while those at ~ 300 meV are due to the Ce $4f_{7/2}^1$ -derived states. The peak structure, just below E_F in CeRhSb, is intense in comparison with that at ~ 300 meV. In the case of CePtSn, the Ce $4f_{5/2}^1$ has almost the equivalent height as that of Ce $4f_{7/2}^1$. These observations seem to be consistent with higher T_K of CeRhSb than that of CePtSn based on the SIAM.²⁵ It is noteworthy, on the other hand, that the peak structure near E_F is fully absent in the spectrum of CeRhAs.

In order to estimate the spectral density-of-states (SDOS), we divided the photoemission spectra (normalized at ~ 300 meV) by a Fermi-Dirac distribution (FDD) function, convoluted with a Gaussian which represents the instrumental resolution,²⁶ as shown in Fig. 3. The resulting spectra are assumed to give the SDOS broadened with the instrumental resolution. One notices again that CeRhAs exhibits quite different spectral features as compared with those of CeRhSb and CePtSn. There is no KR at E_F . The spectral intensity decreases monotonically above ~ 90 meV, forming a large gap structure. It is remarkable that the energy gap of CeRhAs is very close to a fullgap rather than a pseudogap.

As shown in Fig. 3, some differences become apparent near E_F , especially between CeRhSb and CePtSn. In the

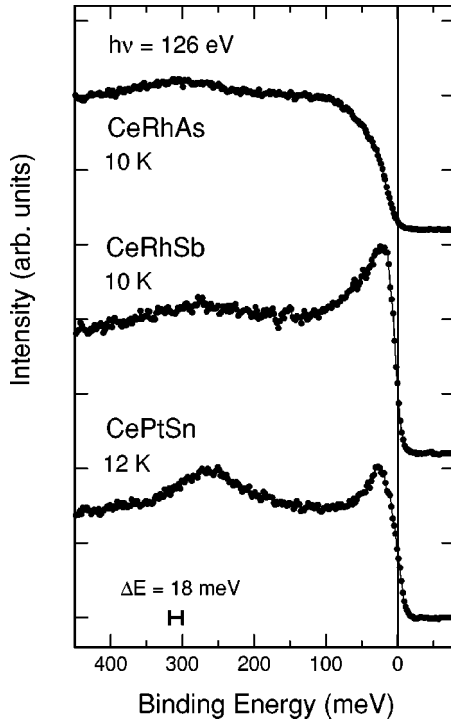


FIG. 2. High-resolution photoemission spectra of CeRhAs, CeRhSb, and CePtSn near E_F . The spectral intensities are normalized to the intensity of the peak at ~ 300 meV.

case of CeRhSb, the spectral intensity shows enhancement above ~ 120 meV, which is similar to that of Kondo metals with high T_K .²⁵ However, above ~ 13 meV the spectral intensity decreases steeply, which is an important feature different from that of CePtSn and other Kondo metals.^{25,26} The rapid decrease in the spectral intensity strongly supports the existence of a narrow pseudogap. The observed Ce 4f¹ SDOS feature of CeRhSb agrees with the V-shaped pseudogap in the conduction bands as proposed in the analyses of the specific heat⁹ and $1/T_1$ of the NMR (Ref. 10) measurements. It is also noted that the size of the pseudogap ~ 13 meV coincides well with the Δ_{p-p} values of 10–13.5 meV obtained by tunneling spectroscopy.⁸

The spectral intensity of CePtSn exhibits no remarkable enhancement near E_F , except for a peak structure at ~ 27 meV. The peak structure is in good agreement with crystal field excitations observed in inelastic neutron scattering.¹⁸ A weak KR is consistent with either the low $k_B T_K < 1$ meV, or a weak $c-f$ hybridization.²⁵ The spectral features of CePtSn can be well interpreted within the framework of the SIAM.

If we compare the present spectra for CeRhAs and CeRhSb single crystals with the He II α -He I α difference spectra obtained for scraped polycrystalline samples,¹² significant differences are noticeable. First, we found no peak structure at E_F in CeRhAs. Second, a very narrow pseudogap exists in CeRhSb. There is no reason to estimate Δ_f by the peak position in the difference spectra.¹² If we evaluate Δ_f by the binding energy from which the Ce 4f SDOS starts to decrease, Δ_f 's are ~ 90 meV and ~ 13 meV for CeRhAs and CeRhSb, respectively.

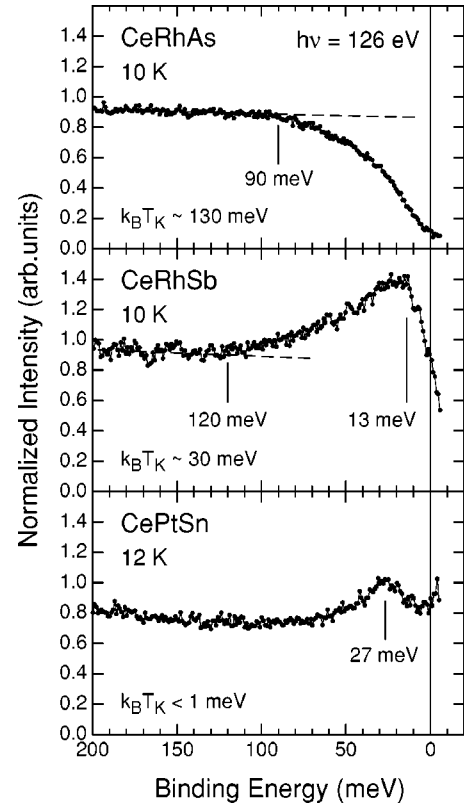


FIG. 3. Photoemission spectra of CeRhAs, CeRhSb, and CePtSn divided by a broadened FDD function. These spectra are assumed to reflect the SDOS broadened with the instrumental resolution. The SDOS of CeRhAs decreases monotonically above ~ 90 meV, forming a large energy gap. The SDOS of CeRhSb enhances above ~ 120 meV but decreases above ~ 13 meV, forming a pseudogap. The SDOS of CePtSn has weak KR, and a peak at ~ 27 meV corresponding to crystal field excitations.

As shown explicitly in Fig. 3, the spectral features at E_F of CeRhAs, CeRhSb, and CePtSn are characteristic of a semiconductor, a semimetal, and a metal, respectively. The Ce 4f electronic states at low temperature in CeRhAs and CeRhSb cannot be explained within the framework of the SIAM, in which the intensity of KR should scale with T_K .²⁵

In order to describe the spectra for CeRhAs and CeRhSb, the PAM or KLM may provide us with an insight into the $c-f$ hybridization near E_F . Based on the PAM, Ikeda and Miyake (IM) presented an anisotropic $c-f$ hybridization model of the ϵ -TiNiSi-type Kondo semimetal CeNiSn in which the conduction bands hybridize with the f state for a particular symmetry of the crystal-field states.²⁷ Moreno and Coleman (MC) extended these considerations by accounting for fluctuations into the f^2 state, and showed that the anisotropic $c-f$ hybridization gap could be modeled, even though the crystal-field splittings were absent.²⁸

The results of IM and MC show a semimetallic single-particle spectral function.^{27,28} In the MC model, the V-shaped spectral density was more pronounced,²⁸ which is closer to the observed spectral shape for CeRhSb. Since the dispersion of the Ce 4f states is assumed to be small in the PAM, it leads to a sharp peak structure near E_F . In addition, the

magnitude of the c - f hybridization (pseudo)gap is decreased, and the spectral density for the Ce $4f$ state becomes narrow due to renormalization effects.^{3-5,27,28} Although the IM and MC models^{27,28} assume rather simple energy-band structures, as compared with that given by full band-structure calculations,^{29,30} the observed spectrum for CeRhSb can be qualitatively understood in terms of these models.

However, with regards to the Kondo semiconductor CeRhAs the situation is quite different. The absence of a peak structure near E_F is highly suggestive of a much stronger c - f hybridization. More realistic energy band dispersions should be taken into account. The observed spectral feature of CeRhAs is significantly different from the spectral function given by the PAM. For future considerations, it is desirable to compare the spectral features with the density-of-states given by band-structure calculations.³¹

In summary, we have investigated the Ce $4f$ -derived electronic states of the isostructural single crystalline CeRhAs, CeRhSb, and CePtSn in the ground state, by utilizing high-

resolution, low-temperature resonant photoemission spectroscopy. The spectral intensity of the Kondo semiconductor CeRhAs monotonically decreased above ~ 90 meV. The spectral feature considerably differs from what the PAM predicted so far. The observed SDOS of the semimetal CeRhSb enhanced above ~ 120 meV but decreased above ~ 13 meV, which can be well described based on the PAM. The spectral features of the metal CePtSn are well explained within the framework of the SIAM with low T_K .

This work was supported by a Grant-in-Aid for COE Research (13CE2002) by the Ministry of Education, Science, and Culture of Japan. We thank the Cryogenic Center, Hiroshima University for supplying liquid helium. K.S. thanks Prof. T. Ekino and Mr. Takasaki for the scanning electron microscope measurements. The synchrotron radiation experiments have been done under the approval of HSRC (Proposal No. 01-A-24).

-
- ¹T. Takabatake *et al.*, *J. Magn. Magn. Mater.* **177-181**, 277 (1998).
²Z. Fisk *et al.*, *Physica B* **206-207**, 798 (1995).
³A.C. Hewson, *The Kondo Problem to Heavy Fermions* (Cambridge University Press, Cambridge, 1993) Chap. 10.
⁴A. Georges *et al.*, *Rev. Mod. Phys.* **68**, 13 (1996).
⁵H. Tsunetsugu, M. Sigrist, and K. Ueda, *Rev. Mod. Phys.* **69**, 809 (1997).
⁶T. Takabatake *et al.*, *Physica B* **206-207**, 804 (1995); **223-224**, 413 (1996).
⁷T. Sasakawa *et al.* (unpublished).
⁸T. Ekino *et al.*, *Phys. Rev. Lett.* **75**, 4262 (1995); *Physica B* **223-224**, 444 (1996).
⁹S. Nishigori *et al.*, *J. Phys. Soc. Jpn.* **65**, 2614 (1996).
¹⁰K. Nakamura *et al.*, *J. Phys. Soc. Jpn.* **63**, 433 (1994).
¹¹H. Kumigashira *et al.* *Phys. Rev. Lett.* **82**, 1943 (1999).
¹²H. Kumigashira *et al.*, *Phys. Rev. Lett.* **87**, 067205 (2001).
¹³J.J. Yeh, *Atomic Calculation of Photoionization Cross-Sections and Asymmetry Parameters* (Gordon and Breach, New York, 1993).
¹⁴C.R. Brundle, *J. Vac. Sci. Technol.* **11**, 212 (1974).
¹⁵Scanning electron microscope images of scraped surfaces indicated many scratches along the traces of a diamond file. Many fragments of the order of $\sim \mu\text{m}$ size stuck on the scraped surface, leading to bad thermal and electrical contacts. The images of the fractured surfaces exhibited appreciably wide and flat areas, and had almost no fragments left.
¹⁶If we compare photoemission spectra obtained from scraped and fractured surfaces, the former have (1) a stronger spectral weight of the Ce $4f^0$ component than that of the Ce $4f^1$ component for all of the present samples, (2) no enhanced peak structure and no pseudogap structure near E_F for CeRhSb, and (3) a smaller reduction of the spectral intensity above ~ 90 meV for CeRhAs.
¹⁷T. Takabatake *et al.*, *Physica B* **183**, 108 (1993).
¹⁸M. Kohgi *et al.*, *Physica B* **186-188**, 409 (1993).
¹⁹N.E. Bickers, D.L. Cox, and J.W. Wilkins, *Phys. Rev. Lett.* **54**, 230 (1985).
²⁰P. Salamakha *et al.* *J. Alloys Compd.* **313**, L5 (2000).
²¹K. Shimada *et al.*, *Nucl. Instrum. Methods Phys. Res. A* **467-468**, 517 (2001); *Surf. Rev. Lett.* (to be published).
²²The crystal momenta of CeRhAs, CeRhSb, and CePtSn are 0.8–1.5, 0.8–1.4, and 0.8–1.2 \AA^{-1} , respectively. With the present experimental configuration, and with the kinetic energy of a photoelectron of ~ 120 eV, the photoemission spectra are averaged over 80–150 % of the Brillouin zone (BZ) along the slit direction, and 20–40 % of the BZ perpendicular to the slit direction.
²³See for example, S. Hüfner, *Photoemission Spectroscopy* (Springer-Verlag, Berlin 1995), Chap. 3.
²⁴See for example, E. Weschke *et al.*, *Phys. Rev. B* **44**, 8304 (1991); H.-D. Kim *et al.*, *ibid.* **56**, 1620 (1997); T. Iwasaki *et al.*, *ibid.* **61**, 4621 (2000).
²⁵M. Garnier *et al.*, *Phys. Rev. Lett.* **78**, 4127 (1997).
²⁶F. Reinert *et al.*, *Phys. Rev. Lett.* **87**, 106401 (2001).
²⁷H. Ikeda and K. Miyake, *J. Phys. Soc. Jpn.* **65**, 1769 (1996).
²⁸J. Moreno and P. Coleman, *Phys. Rev. Lett.* **84**, 342 (2000).
²⁹A. Yanase and H. Harima, *Suppl. Prog. Theor. Phys.* **108**, 19 (1992).
³⁰T.J. Hammond *et al.*, *Physica B* **206-207**, 819 (1995).
³¹J.-S. Kang *et al.* *Phys. Rev. B* **60**, 5348 (1999); A. Sekiyama *et al.*, *Solid State Commun.* **121**, 561 (2002).